CHALMERS
UNIVERSITY OF TECHNOLOGY

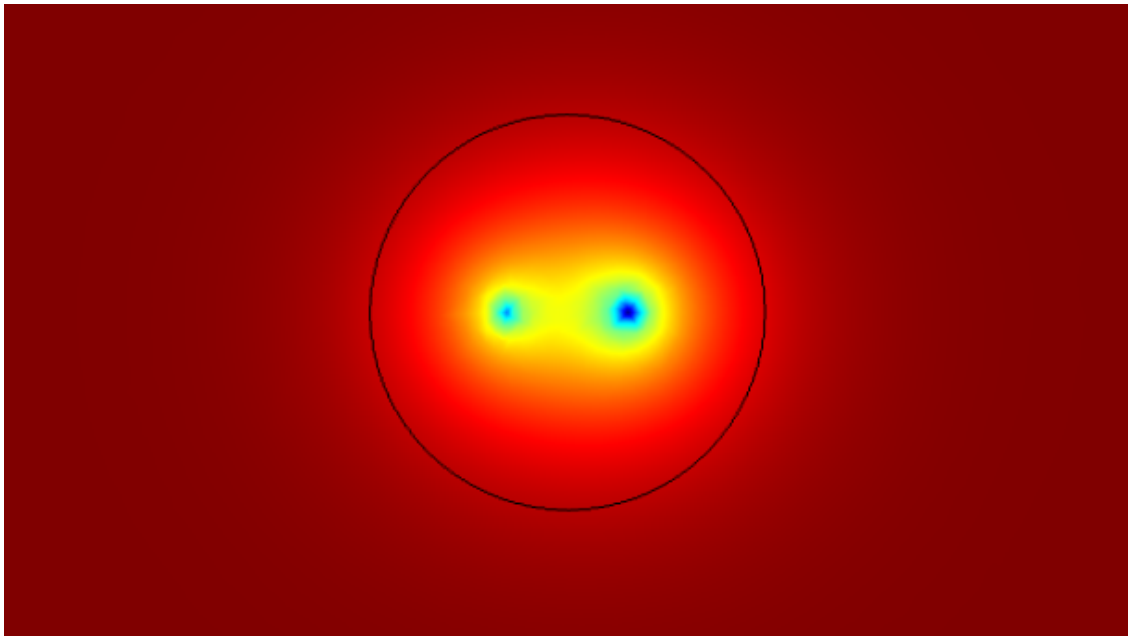

Thermodynamic Assessment of a Deep Geothermal Heat Pump System

Master's Thesis in Sustainable Energy Systems

JAKOB WADSTEIN

Department of Space, Earth and Environment
CHALMERS UNIVERSITY OF TECHNOLOGY
Gothenburg, Sweden 2019

Master's thesis 2019

Thermodynamic Assessment of a Deep Geothermal Heat Pump System

JAKOB WADSTEIN

CHALMERS
UNIVERSITY OF TECHNOLOGY

Department of Space, Earth and Environment
Division of Energy
Chalmers University of Technology
Gothenburg, Sweden 2019

Thermodynamic Assessment of a Deep Geothermal Heat Pump System
JAKOB WADSTEIN

Supervisor: Fredrik Normann, Department of Space, Earth and Environment,
Lars Strömberg, CEO Vasa Värme, Professor Emeritus at Chalmers University of Technology
Examiner: Filip Johnsson, Department of Space, Earth and Environment

Master's Thesis 2019
Department of Space, Earth and Environment
Division of Energy
Chalmers University of Technology
SE-412 96 Gothenburg
Telephone +46 31 772 1000

Cover: Temperature spread from boreholes in xy-plane, cut at z -2000 m.

Typeset in LaTeX
Gothenburg, Sweden 2019

Thermodynamic Assessment of a Deep Geothermal Heat Pump System
Jakob Wadstein
Department of Space, Earth and Environment
Chalmers University of Technology

Abstract

Current geothermal energy exploitation is confined to porous, water saturated sedimentary rock. Excluding a few small scale industrial and research complexes, little progress has been made to reach the underlying crystalline bedrock, called hot dry rock (HDR). The potential of this resource is considered to be abundant and far outweigh the standard geothermal source in sedimentary bedrock utilized today. The focus of research has so far been in "engineered" HDR, meaning in some way creating a fracture system, through which to circulate water, in the otherwise impermeable bedrock. However, creating this fractured network is a perilous enterprise in several ways. In experimental drilling there have been issues with fluid leaks, induced seismic activity and flow short circuits among others. It is of interest to investigate alternatives in extracting this energy.

This thesis has the ambition to investigate a closed loop geothermal system, consisting of two boreholes connected at a depth of 3500 m in the crystalline bedrock. A model was built using COMSOL Multiphysics 5.3. The rock properties were defined in a way common to Sweden and a heat pump is considered to be connected to the system, allowing for a constant temperature of the fluid returning to the surface. The purpose of the study was to discern which parameters that were affecting the energy extraction and how. With that goal in mind, fluid flow, incoming fluid temperature, borehole radius and thermal conductivity of the crystalline bedrock were alternated in a series of simulations. Fluid flow and incoming fluid temperature are operational phase values and are the only conditions which can be altered after construction of the system. Borehole radius has a strong impact on drilling cost. The thermal conductivity of the bedrock is a site specific value and changing this exposes the impact of more or less preferable subsurface conditions. The results shows that the convection in the boreholes were more than adequate to saturate the heat exchange with its surroundings. Limiting factors proved to be the temperature gradient between borehole and bedrock, together with rock thermal conductivity. The high thermal inertia of the bedrock, which signifies how slowly the temperature of a section of rock reaches that of its surroundings, and the relatively low thermal conductivity failed to supply adequate heat, resulting in a rapid decline in energy extraction, in the first few years of operation. Thus the heat penetration in the bedrock limits the possible thermal power output.

Keywords: geothermal, crystalline bedrock, thermal conductivity, thermal inertia, conduction, convection, HDR.

Acknowledgements

I would like to thank my supervisor Fredrik Normann and my examinor Filip Johnsson for their continued support during the long and testing journey this Masters' Thesis proved to be. I also extend a big thank you to Lars Strömberg CEO of the company Vasa Värme and Professor Emeritus at Chalmers University of Technology, who provided the Thesis proposal and gave invaluable direction throughout its process.

Jakob Wadstein, Gothenburg, December 2018

Contents

List of Figures

List of Tables

1
Introduction

1.1 Background

Until the beginning of the 20th century, geothermal energy was mostly used for recreational purposes and minor heating services. With the advancement of technology and the increased demand for electricity, the use of geothermal energy was recognized and large scale exploitation began. However, even though the geothermal technology has developed, it has a weak standing among the more conventional renewable energy sources despite having great potential to alleviate our strong dependency on fossil, and other non-renewable fuels[1]. Outside of geothermal hot-zones, this resource has had a slow development for larger scale production. For most low enthalpy zones, also known as zones with a low temperature gradient, relatively few large geothermal systems is currently in operation.

Besides the temperature gradient there are two more major factors in geothermal exploitation. These are rock permeability and presence of fluids[2]. As of now the dominating part of geothermal extraction is performed in areas where all three factors are favourable[3]. These parameters make it possible to extract water with an adequate temperature for direct use in heating or electricity production. This source is called conventional hydrothermal resource and can already provide electricity at competitive prices in countries such as Italy, Iceland and Turkey[4]. Unfortunately, most geothermal energy available is present in deep lying crystalline bedrock, lacking in water and rock permeability[5], which create challenges in how to efficiently extract the energy within. These resources are know as Hot Dry Rock (HDR). The research into this form of geothermal energy, which is completely different from conventional geothermal resources, is only a few decades old and has had a slow development. The hindrance for energy extraction is the depth of the resource, typically several kilometers below surface, and the compact bedrock. The idea for tapping into HDR is generally to create an artificial permeability, by breaking up the rock through fracking or to use chemicals to dissolve minerals. This would create a network of cracks where it would we possible to circulate fluid between two wells. Due to the stochastic nature of "engineering" this kind of geothermal system, the outcome of such an endeavour is uncertain[6] and the last few decades of development have been mostly experimental. An alternative solution could be a closed loop system of two boreholes, connected a few kilometers below ground in the crystalline bedrock creating a borehole heat exchanger. Such a system corresponds to a simpler design and possibly give a more predictable way to access the vast potential of HDR.

Knowledge of geomechanics has made good progress, in large part due to fossil fuel extraction[5]. However, circumstances under these conditions are often inconsistent with those encountered, when geothermal interests are the main priority. This makes for a weak connection between the geomechanical branch, rock mechanics research and the geothermal industry. Understanding of rock mechanics in the planning and execution of geothermal projects is becoming increasingly important, in maximizing conventional geothermal resources and for the development of engineered geothermal systems. Because of this, there exists a gap between the geomechanical and geothermal communities, hampering the progress of geothermal technologies.

This Master's Thesis was proposed by the company Vasa Värme. The company owns several district heating (DH) networks and biomass based heat production facilities scattered throughout Sweden. Striving for sustainability, they are interested in researching and incorporating geothermal energy with DH networks through heat pumps. Generally, Sweden has a relatively thin sedimentary layer followed by crystalline bedrock, with an unfavourable geothermal gradient, making it less lucrative to tap into natural aquifers. This means that most of Sweden's geothermal energy potential is matched to the relatively unexploited category of crystalline bedrock, where the major potential future of geothermal energy exists.

The exploitation of this resource is connected to progress in water hammer drilling techniques, which have made it cheaper and easier to drill deeper into the crystalline bedrock. This opens up opportunity to reach depths, able to provide temperatures suitable for DH with heat pumps even in unfavourable conditions. At the time of writing this thesis, experimental drilling at deeper depths is performed but limited. Besides a large investment cost, heat produced in this fashion has a low variable cost and it is close to free from carbon dioxide. These two arguments give a strong incentive to evaluate the feasibility and profitability of this technology.

1.2 Aim

To achieve knowledge and understanding of the difficulties in implementing a closed loop HDR geothermal system, an important step is to build a mathematical model and simulate how a typical system could function and what results are to be expected. For this purpose, the software COMSOL Multiphysics[1] has all the tools necessary to describe the complex coupling of the different physics required in this kind of problem. The goal was to build and analyze a model of a deep geothermal heat pump in Swedish conditions. The base case scenario is provided by Vasa Värme and involves two boreholes connected 3.5 kilometers below ground in the crystalline bedrock, allowing water to circulate and heat up during its time underground. The incoming water temperature is set to 18 $^{\circ}C$, to allow for a fair coefficient of performance (COP) when connected to a heat pump, with the purpose of providing heat

[1] https://www.comsol.com/

to a district heating system. For a temperature gradient of 0.015 K/m, the depth needed for a direct use of the return water in district heating is close to 7 km. As of now this depth is outside of conventional drilling and the borehole depth is therefore limited to 3.5 kilometers. In the interest of long term return on the investment associated with the construction of a geothermal plant, the simulations run over 30 years. The aim is to analyze the extraction of energy, to see what parameters that are affecting the results and how. With this aim in mind, the system will be tested by changing rock thermal conductivity, fluid mass flow, incoming fluid temperature and borehole radius.

1.3 Delimitations

Economic analysis is not to be in the scope of this Master Thesis. A thermal gradient of 15 K/km is chosen since the range in Sweden is 15-30 K/km [2], where the higher gradients are confided to the southernmost part of the country. No aquifer is assumed to be present at depths relevant to this study and will thus be left out in modelling cases. The system at this depth is considered to be impermeable, with the boreholes enclosed in steel casing, thus not accounting for any water loss. Optimization of the system is not included, but the pure behaviour and trends are to be analyzed.

[2] https://www.sgu.se/samhallsplanering/energi/fornybar-geoenergi-och-geotermi/geotermi/

2
Theory

The theory part consists of fluid and solid physics together with its simplifications and application in the software COMSOL Multiphysics pipe module. Properties of the bedrock types are also included.

2.1 Fluid physics

There are three main parts governing the study of heat and fluid flow. They are the continuity equation, the equations of momentum and the equation of continuity of energy. Used in a broad range of applications and circumstances, although all seemingly different and specified to the certain problem, they originate from the same basic principles. Namely, the principle that mass, energy and momentum cannot simply disappear, Newton's law of motion and the laws of thermodynamics[7].

2.1.1 COMSOL Multiphysics simplifications for pipe flow to governing equations

Derived from the Navier-Stokes equations it is possible to obtain a set of equations, describing the quasi-one dimensional behaviour of a fluid in a tube. Shown by C.L. Barnard et al.[8] the basic continuity and momentum equations of fluid flow is simplified in COMSOL Multiphysics and described in the following way:

$$\frac{\partial A\rho}{\partial t} + \nabla \cdot (\rho A\mathbf{u}) = 0 \tag{2.1}$$

and

$$\rho\frac{\partial \mathbf{u}}{\partial t} = -\nabla p - f_D\frac{\rho}{2d_h}\mathbf{u} \mid \mathbf{u} \mid +\mathbf{F} \tag{2.2}$$

$\mathbf{u}$ (m/s) is the cross-section averaged velocity, p (Pa) is pressure, ρ (kg/m^3) is density, f_D is the dimensionless Darcy friction factor and $\mathbf{F}$ (N/m^3) is the volume force term. d_h (m) is the mean hydraulic diameter defined as:

$$d_h = \frac{4A}{Z} \tag{2.3}$$

A (m^2) is the cross section area and Z (m) is the wetted perimeter.

The second term on the right hand side of equation 2.2 represents pressure loss due to friction. Churchill equation for describing the Darcy friction factor is standard in the COMSOL Multiphysics module *Pipe Flow*. It is widely accepted and usable for a wide range of Reynolds numbers in all types of flow, laminar, transition and turbulent. It is expressed in the following manner:

$$f_D = 8[(\frac{8}{Re})^{12} + (A+B)^{-1.5}]^{1/12} \tag{2.4}$$

$$A = [-2.457ln((\frac{7}{Re})^{0.9} + 0.27(e/d))]^{16} \tag{2.5}$$

$$B = \left(\frac{37530}{Re}\right)^{16} \tag{2.6}$$

with e as dimensionless surface roughness and d as diameter (m).

Further simplification is done in the COMSOL Multiphysics module by introducing a tangential vector.

$$\mathbf{e}_t = (e_{t,x}e_{t,y}e_{t,z}) \tag{2.7}$$

Adding this to the momentum equation:

$$\mathbf{e}_t\left[\rho\frac{\partial \mathbf{u}}{\partial t} = -\nabla p - f_D\frac{\rho}{2d_h}\mathbf{u} \mid \mathbf{u} \mid + \mathbf{F}\right] \tag{2.8}$$

Since all velocity components perpendicular to the axial flow is assumed to be 0, the tangential velocity u can be defined as $\mathbf{u} = u\mathbf{e}_t$. The tangential velocity is the quantity solved by the module *Pipe Flow* in COMSOL Multiphysics.

For the energy equation, COMSOL Multiphysics uses the form from M.V. Lurie [9] and the equation is adapted to a 1D pipe flow, taking into account the tangential velocity, which was previously defined.

$$\rho AC_p\frac{\partial T}{\partial t} + \rho AC_p\boldsymbol{u}\cdot\nabla T = \nabla\cdot Ak\nabla T + f_D\frac{\rho A}{2d_h} \mid \mathbf{u} \mid^3 + Q + Q_{wall} \tag{2.9}$$

Here C_p $(J/(kg\cdot K))$ is heat capacity at constant pressure, ρ (kg/m^3) is fluid density, T (K) is temperature, k $(W/(m\cdot K))$ is thermal conductivity and $\mathbf{u}$ (m/s) is the velocity field, see the momentum equation2.2. This equation has several terms included which is not in the standard engineering fashion. Second term on right hand side is heat generated by shear stress with the boundary wall. Third term on the right hand side Q (W/m) represents a heat source in the element and the last term Q_{wall} (W/m) stands for heat exchange though the pipe wall.

Expanding the heat exchanging term Q_{wall} for further explanation:

$$Q_{wall} = (hZ)_{eff}(T_{ext} - T) \tag{2.10}$$

Z(m) is the perimeter of the pipe, $(hZ)_{eff}$ $(W/(m^2 \cdot K))$ is the effective overall heat transfer coefficient and T_{ext} is external temperature of the pipe. T_{ext} can be defined in COMSOL Multiphysics in several different ways, constant value, parameter etc. In this situation the external temperature is modeled as a 3D field, represented by the ambient bedrock. The coupling between the pipe and surrounding volume is done by representing the pipe as a line heat source/sink in the 3D domain.

2.1.2 Overall heat transfer coefficient

A crucial factor in heat exchanger design is the overall heat transfer coefficient. It controls the viable attribution of the term Q_{wall} (Eq: 2.10), which describes heat exchange between the fluid in the pipe and its surroundings. Naturally, for any heat exchange to occur there must be a temperature difference, as is shown in the equation, but the rate or efficiency of this exchange is controlled by the $(hZ)_{eff}$. As defined in COMSOL Multiphysics, the value of the heat transfer coefficient multiplied by the pipe perimeter. For a pipe the effective hZ can be described as:

$$(hZ)_{eff} = \frac{2\pi}{\frac{1}{r_0 h_{int}} + \frac{1}{r_N h_{ext}} + \sum_{n=1}^{N}(\frac{ln(\frac{r_n}{r_{n-1}})}{k_n})} \tag{2.11}$$

The first term in the denominator stands for internal film resistance, the second for external film resistance and the sum term stands for the different wall layers of the pipe. The overall heat transfer coefficient is affected by several factors; the internal film resistance, wall resistance, and external film resistance. For a pipe buried in crystalline bedrock, the outer film resistance can be neglected due to the absence of fluid. Closer to the surface of the earth, the possibility exists for the presence of a ground water reservoir. The length of pipe assumed to be affected by this is small compared to the total length of the pipe (sec: 2.3), and will be neglected in this thesis.

A descriptive image of the cross-section of a pipe with a arbitrary number of wall layers (fig: 2.1), showing the temperature range from the inside of the pipe all the way to the outer perimeter. In the current case heat is shown to be flowing from the pipe fluid to the outer volume, however the physics and rules apply in the same way to the reverse situation. Breaking down equation 2.11 for better understanding of the underlying parameters, there are two equations used. The first describes the inside and outside film resistance, and the second is for the different pipe layers. A short length of the pipe ∇L is introduced and $A = \nabla L 2\pi r$ is defined as heat transfer area.

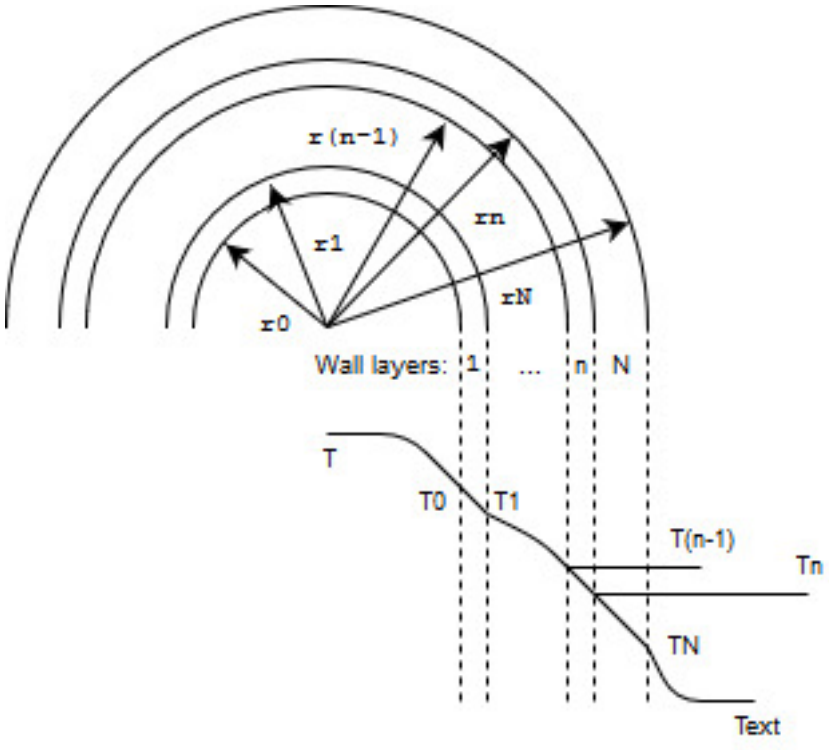

Figure 2.1: Cross-section of pipe

$$Q_{wall} = h_{film} A (T - T_{film}) \tag{2.12}$$

and

$$Q_{wall} = \nabla L 2\pi r \Big(- k_n \frac{dT}{dr} \Big) \tag{2.13}$$

The rate of convective heat transfer is described by Newton's law of cooling also Newton rate equation:

$$q = hA\triangle T \tag{2.14}$$

Here q is convective heat transfer (W), A (m^2) is area perpendicular to the direction of the flow and h is convective heat transfer coefficient (W/m^2) and $\triangle T$ is temperature difference (K).

2.1.3 Reynolds number and entry region

For flow in circular tubes the Reynlods number is defined as:

$$Re_D \equiv \frac{\rho u_m D}{\mu} = \frac{u_m D}{\nu} \tag{2.15}$$

Where ρ is density (kg/m^3), μ is the dynamic viscosity of the fluid ($kg/(m \cdot s)$), u_m is the mean fluid velocity over the tube cross section and D is the tube diameter.

For flow in pipes a Reynolds number of 2300 is considered to be the critical point, where laminar flow transcends to turbulent flow although the transition regime is normally defined in the range of $10^3 < Re < 10^4$. Around this number we have the transition flow containing both laminar and turbulent flow. However, in most engineering problems, circumstances (fluid, velocity, pipe material and geometry) makes turbulent flow most common and thus more relevant to study[10]. Turbulent flow is the state of the liquid in this Master's Thesis.

For flow in circular tubes the entry length before fully developed turbulent flow is largely independent of the Reynolds number[11] and an approximate length can be derived as:

$$10 \leq (\frac{x_{fd,h}}{D})_{turb} \leq 60 \tag{2.16}$$

For long tubes the transition region is usually neglected due to its low impact in long tubes and a fully developed turbulent region is assumed for the entirety of the tube. COMSOL Multiphysics module *Pipe Flow* assumes a fully developed region.

2.1.4 Velocity and thermal profiles

With the assumption of fully developed turbulent flow in the entire tube, a simplification regarding fluid velocity is possible. Due to the variation of velocity over the tube cross section that the turbulent flow entices, together with the lack of a free stream velocity, the standard approach in tackling internal flow is to use the mean velocity u_m[11]. This means no regard will be given to the impact of the velocity profile in the calculations.

In the same way that velocity creates a velocity profile, temperature develops a temperature profile due to convection in the tube. The shape of this profile differs depending on fluctuations in surface temperature and heat flux. Before a fully developed thermal profile there exists a thermal entry length working under similar conditions as velocity. However, unlike the velocity this entry length is dependant on the Prandtl number for laminar flow:

$$(\frac{x_{fd,t}}{D})_{lam} \approx 0.05 Re_D Pr \tag{2.17}$$

For turbulent flows the thermal entry length is largely independent of the Prandtl number, giving a similar simplification of the entry length as for velocity $(x_{fd,t}/D) = 10$[11]. In the same way as for velocity in turbulent flow, the use of a mean temperature is practical due to the lack of a fixed free stream temperature. It refers to the simplified steady-flow thermal energy equation, where T is assumed to be uniform over the cross section, which of course does not reflect reality properly:

$$q = \dot{m} c_p (T_{out} - T_{in}) \tag{2.18}$$

To accommodate for this the temperature is integrated over the tube cross section giving the mean temperature T_m:

$$T_m = \frac{2}{u_m r_o^2} \int_0^{r_o} uTrdr \tag{2.19}$$

A constant density and specific heat capacity is assumed. The mean temperature gives a convenient reference when calculating internal flow.

2.2 Solid physics

Considerably simpler with respect to fluid physics, the COMSOL Multiphysics *Heat Transfer in Solids* module uses the following equation for heat transfer:

$$\rho C_p \frac{\partial T}{\partial t} - \nabla \cdot (k \nabla T) = Q \tag{2.20}$$

With ρ (kg/m^3) density, C_p $(J/(kg \cdot K))$ heat capacity, k $(W/(m \cdot K))$ thermal conductivity and Q (W) which is a heat source.

2.3 Bedrock

The bedrock is divided into two parts aimed to simulate a thin sedimentary rock layer followed by crystalline bedrock. The parts of the boreholes calculated to be emerged in sedimentary rock is considered to be lined with thin steel casings 1 mm thick. This is to simulate the actual scenario where there is a need to separate the boreholes from the porous rock, to avoid contamination of production fluids and groundwater. In the crystalline bedrock this is lesser of an issue since the rock porosity mainly consists of microfractures[12] and the presence of these inconsistencies decline rapidly with depth[6]. There is a heat source in the rock itself due to the decay of radioactive isotopes amounting to 2.47 $\mu W/m^3$. This heat source is small but it is included to more closely mimic the conditions in the bedrock.

2.3.1 Sedimentary rock

The upper part of the model represents the layer of sedimentary rock. The heat conduction for this part is difficult to estimate, since the local conditions regarding rock type and groundwater is site specific.

For limestone, slate and sandstone the range of heat conduction is 1.8 - 6.2 $W/(m \cdot K)$ [13]. As a base case, for the purpose of comparison in this Master's thesis, a value of 3.5 $W/(m \cdot K)$ was chosen. This is consistent with the heat conduction of the granite crystalline bedrock. Along the borehole pipe walls there is also the presence of a casing, which separates the pipe fluid from the rock wall. For the purpose of simulating this effect in COMSOL Multiphysics, the additional thin steel casing

layer will be poor heat isolation. With heat conductivity in the range of 16 - 54 $W/(m \cdot K)$ from stainless steel to carbon steel. Even though no ground water is simulated in the model this extra layer is added for additional realism.

2.3.2 Crystalline rock

The larger lower part of the bedrock represents the crystalline granite most common to Sweden. At a depth of 300 m, the properties of the model volume takes on the characteristics of the granite, which stretches down to the end of the model. Porosity have an impact on thermal conductivity of rock as shown by Cho et al.[14]. However, porosity concerns are mainly a subject of discussion when dealing with sedimentary rock, related to the void caused by pores. In crystalline rock the porosity is generally low[12] and it predominantly consists of microfractures. The most important factor affecting the thermal conductivity in crystalline rock, is the mineral composition present[15]. For granite the major minerals are quartz and albite. Of these quartz has the highest thermal conductivity at 7.7 $W/(m \cdot K)$. Sweden's granite bedrock consists of 20-40 % quartz and the average thermal conductivity is 3.5 $W/(m \cdot K)$[13].

3
Methods

In this thesis, a numerical analysis model was developed to evaluate the possible thermal power output and thermal behavior of a closed loop deep geothermal heat pump. COMSOL Multiphysics was the software chosen for the modelling and simulation. Using chosen software, a model was constructed of a geothermal heat exchanger system, with the basic structure of two boreholes, connected 3500 m below ground in the crystalline bedrock, with water entering the system at a constant temperature and water flow. Incoming temperature and water flow are two parameters which are under the operators' control, and a certain amount of effort was allocated for sensitivity analysis of these. Outside of the parameters possible for manipulation by operators, thermal properties of the bedrock where also included in the analysis together with borehole radius.

3.1 COMSOL Multiphysics 5.3a

For the purpose of the thesis a modelling software capable of simulating the required physics had to be found. Several candidates are available on the market such as FEFLOW[1] or TOUGH2[2] however, most programs are leaning towards modelling of groundwater flow and its interactions with geothermal systems. COMSOL Multiphysics 5.3a[3] also has these kinds of features, at the very least making it equal to its competitors. However, groundwater simulation is not imperative to the current task, where models mainly will be devoid of this feature. Additionally, COMSOL Multiphysics has a special module named *Pipe Flow* [4] which is especially adapted to simulate fluid flow and heat transfer in long pipes, where the flow can be considered fully developed. This is certainly the case in a deep geothermal system where pipe length to radius ratio is extremely large.

For the purpose of modelling a closed loop deep geothermal heat pump in crystalline bedrock, there where two modules needed: *Heat Transfer in Solids* (ht) and a subcategory of the module *Pipe flow*, namely *Nonisothermal Pipe Flow* (nipfl).

[1] https://www.mikepoweredbydhi.com/products/feflow
[2] https://tough.lbl.gov/
[3] https://www.comsol.com/
[4] https://www.comsol.com/pipe-flow-module

3.1.1 Heat Transfer in Solids

This module provides tools for solving a wide array of heat transfer situations. It accommodates for heat transfer through conduction, convection and radiation. It can calculate for conservation of heat and energy balances together with several related phenomenon, often used in collaboration with other physics. This module is used for describing heat transfer in the bedrock and it is the calculated temperature from this module which is the coupling to the *Nonisothermal Pipe Flow* module. Specified in this module is the bedrock materials and their properties, together with initial values of temperature. Possible heat sources can also be added, as a boundary condition or as a attribute of the domain. On all boundaries the appropriate conditions needs to be set, where the options are thermal insulation, open boundaries or a constant value.

3.1.2 Nonistothermal Pipe Flow

This module is specifically developed for thin pipes, where the ratio of length to radius is large enough, so that the flow can be considered fully developed in the entirety of the pipe. It solves for incompressible fluid flow and heat transfer in pipes. It shares the physics with the $PipeFlow$ module, with the added possibility of calculating pipe heat exchange. The module is developed to save computational power by modelling the pipe in 1D, possible to link with 2D and 3D geometries by representation as a boundary (2D) or an edge (3D). The pipe is represented as line and is automatically coupled with the surrounding geometry as a heat source or heat sink depending on the conditions. The external temperature is the input for the heat exchange through the pipe wall.

3.2 System model

A standard scenario is provided by Vasa Värme, which consists of two boreholes drilled 100 m apart, connected below ground at a depth of 3500 km and with borehole radius of 125 mm. The boreholes are lined by thin steel casing of 1 mm. The system is symmetrical and has the shape of a V. Encompassing the boreholes is a 300 m thick sedimentary layer of bedrock followed by crystalline bedrock, which stretches down to the bottom of the model. Incoming fluid temperature is 18 $°C$ and fluid mass flow is 15 kg/s.

The system is considered to operate in Sweden, where rock properties is defined as clarified in Section 2.3. The material properties of focus for the standard scenario, is presented as follows:

Properties\Material	Water	Crystalline bedrock	Sedimentary bedrock
Specific heat capacity	4187 J/(kg*K)	850 J/(kg*K)	760 J/(kg*K)
Density	998 kg/m^3	2600 kg/m^3	2300 kg*m^3
Thermal conductivity	0.6065 W/(m*K)	3.5 W/(m*K)	3.5 W/(m*K)

Table 3.1: Properties of materials in standard scenario

The base model geometric parameters, together with parameters subject of study, is defined as follows in the COMSOL Multiphysics model builder.

Parameters

Name	Expression	Value	Description
h_crys	3600[m]	3600 m	Depth of crystalline rock
w	400[m]	400 m	Side of rock
radius	125[mm]	0.125 m	Radius of pipe
h_pipe	3500[m]	3500 m	Depth of pipes
T_grad	0.015[K/m]	0.015 K/m	Thermal gradient
m_w	15[kg/s]	15 kg/s	Water flow
T_in	291.15[K]	291.15 K	Inflow temperature
h_sed	300[m]	300 m	Depth of sedimentary rock
T_ground	280.15[K]	280.15 K	Average ground temperature
w_boreholes	100[m]	100 m	Surface distance between boreholes
k_crys	3.5 [W/(m*K)]	3.5 W/(m·K)	Thermal conductivity crystalline bedrock
k_sed	3.5 [W/(m*K)]	3.5 W/(m·K)	Thermal conductivity sedimentary bedrock

Figure 3.1: Basic system parameters

In order to create a volume large enough to not affect the result of the simulation, a side of 400 m (x, y) and a depth of -3600 m (z) is modelled. The first 300 m of depth is defined as the sedimentary layer. Thereafter, the volume takes on the characteristics of the crystalline bedrock, which stretches down to the full length of the model. The surface temperature of the model is 10 $°C$, that is to say at z = 0 m. The temperature gradient 0.015 K/m is applied to the volume. Temperature is thereby increasing with a negative z. Due to the ratio of width and height it is difficult to show the geometry in its complete form. The following image shows the upper part of the geometry where the 300 m thick sedimentary layer can be clearly seen, together with a piece of the underlying crystalline geometry. The cylinder, which can be seen in the center of the model, is the predefined domain around the boreholes, needed to refine the mesh as will be explained in subsection 3.3. The line segments representing the boreholes can be spotted in the cylinder.

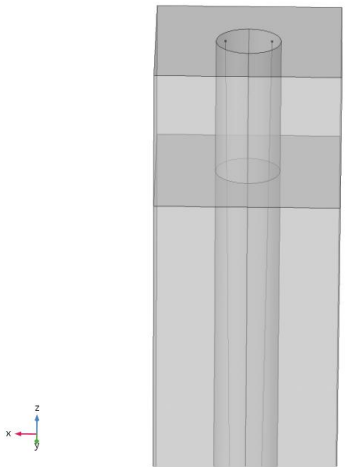

Figure 3.2: Upper part of geometry

3.3 Mesh

When using COMSOL Multiphysics pipe module, the pipe is represented as a 1D line in the ambient 3D domain. Meshing of this line is then controlled by the mesh of the domain, thus there is no need to define a specified mesh for the line itself. Needless to say the mesh of the pipe and the immediate area around it is the most important for the current situation. Since the rock domain can be considered vast compared to the slender structure of the boreholes, it is imperative to have a good mesh control to avoid excessive computational effort. For this purpose the rock domain is split up in an inner and outer area where the inner part encircles the two boreholes in a cylindrical shape. The cylinder has a radius of 70 m, giving at minimum 20 m of distance from domain edge and boreholes.

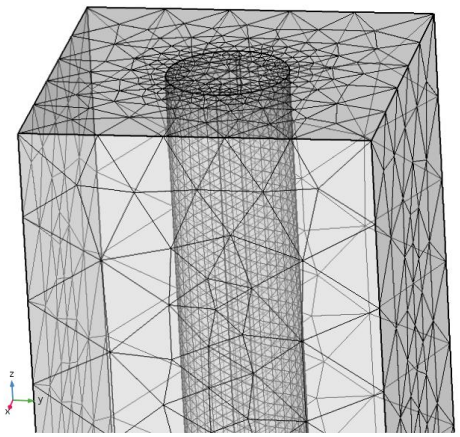

Figure 3.3: Inner mesh

This allows for having a finer mesh close to the boreholes, with a gradual increase in element size until contact with the outer coarser mesh of the surrounding bedrock. The mesh consists of free tetrahedral elements. The number of elements amounts to 324 053 domain elements, 22 630 boundary elements and 1606 edge elements.

3.4 Simulation

First the standard scenario was simulated and displayed as a reference. In order to see which parameters and conditions that impact the system and to what extent, the model was simulated in several different configurations. The design parameter borehole radius was evaluated ranging from a small diameter of 75 mm up to 300 mm. Together with operating parameters fluid mass flow from 1 kg/s to 35 kg/s and incoming water temperature from 0 $°C$ to 35 $°C$. The bedrock properties were also subject to change, with a thermal conductivity from 1 $W/(m \cdot K)$ to 8 $W/(m \cdot K)$. These parameters were subject to individual parametric sweeps, with the remaining values like in the standard scenario. This was to highlight the extent of influence that each parameter had over the system performance as a whole. The simulated time interval was 30 years, to show the longevity of the output. The simulations were continuous, meaning no regard is taken to eventual fluctuations in demand of heating, or other reasons for temporary shutdown of operation.

4

Results

First a sensitivity analysis is carried out to confirm the robustness of the system. The mesh is of special concern and to validate the element size two simulations is performed with higher and lower resolution. When adequate refinement of the mesh is achieved, the standard scenario is simulated. Lastly, the chosen parameters are subject to a series of parametric sweeps. This is an option in COMSOL Multiphysics where the parameter, or parameters in question, are under iterative change to receive a data set, where one can easily switch between the values in the post processing stage.

4.1 Mesh analysis

For the base case model a sensitivity analysis is conducted by increasing and decreasing mesh size by 25 %. The test is carried out with the standard parameters and geometry as described in Chapter 3. The difference in outgoing fluid temperature was chosen as the parameter to analyze. The change showed little influence over the results with 0.08 $degC$ between the finer and coarser mesh sizes.

4.2 Standard scenario

The standard scenario was simulated to display the general behaviour of the system.

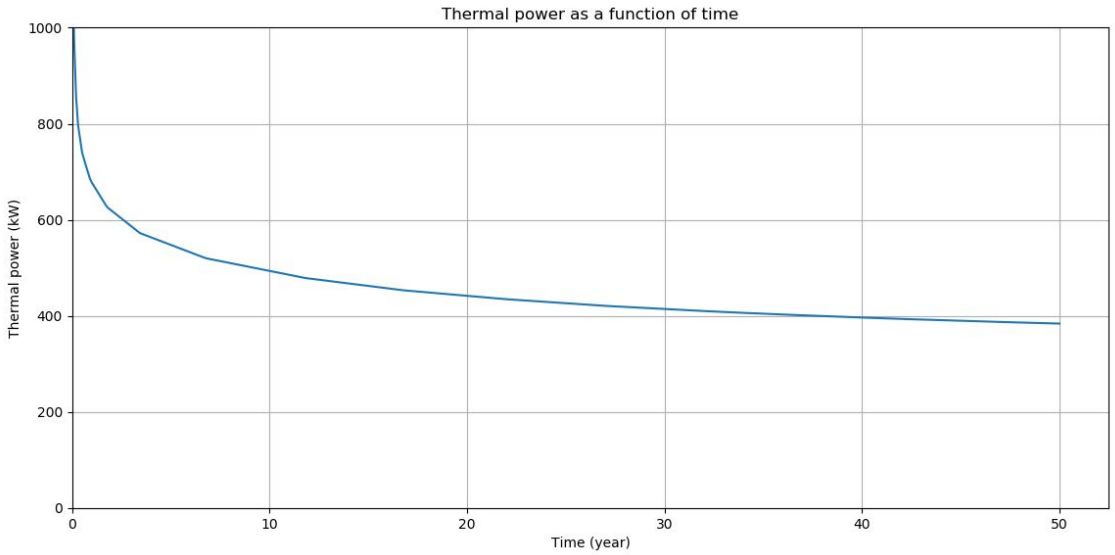

Figure 4.1: Thermal power (kW) as a function of time with standard parameters

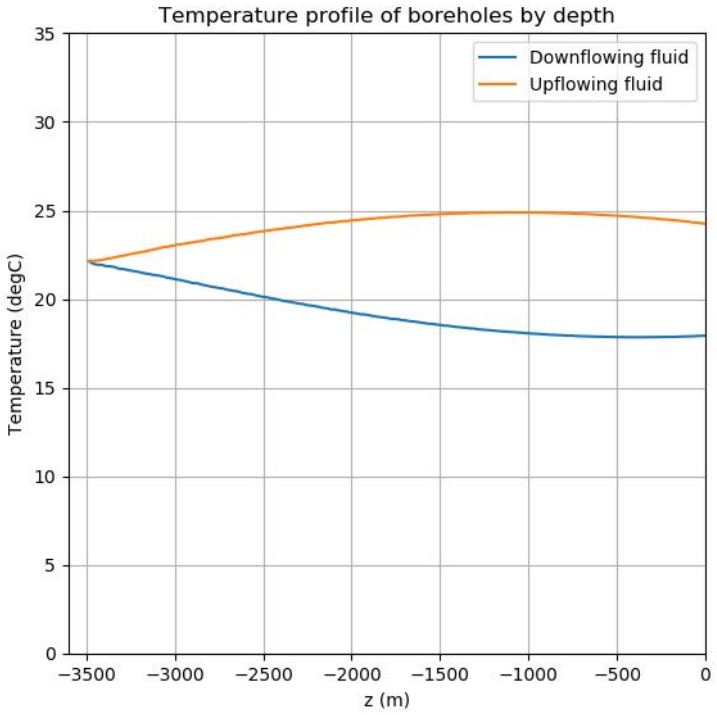

Figure 4.2: Temperature profile ($°C$) in the boreholes after 30 years of operation as a function of depth (m). Blue line is borehole with downflowing water and orange line is borehole with upflowing water.

In figure 4.1 the thermal power output is displayed over time. At year 30 of continuous the thermal power settles at 414 kW and outflowing temperature of 24.6 $°C$. The decline from the initial over 1000 kW is rapid at first but reaches a more

steady state after a few years. With time the thermal power draws closer to a thermal equilibrium with the surrounding bedrock. For this specific simulation the time span was increased to 50 years to further highlight the stability of the curve. At the 50 year point the thermal power has decreased to 384 kW and 24.1 $°C$.

The temperature profile in the boreholes is shown in figure 4.2, with the blue line representing downflowing water and orange line representing upflowing water. The water, initially at 18 $°C$, is first slightly cooled in the upper 397 m of bedrock, before reaching a depth with a positive temperature gradient. The heating of the water is not confined to downward flow but continues after the bend. While it does not gain as much energy in upward flow, the water experiences a positive heat exchange up to a depth of -1083 m. The temperature is then 24.9 $°C$, and it loses 0.6 $°C$ the rest of the way to the surface.

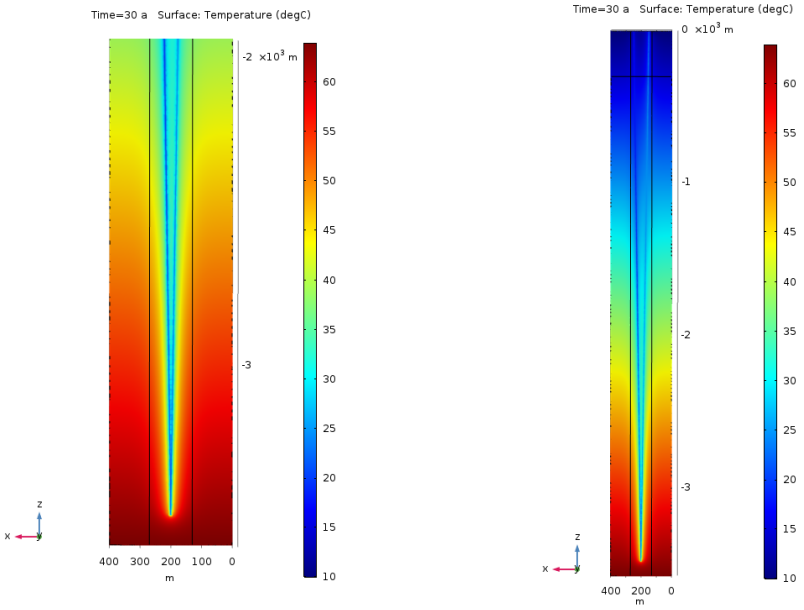

(a) Temperature contour of lower 1600 m

(b) Temperature contour of volume

Figure 4.3: Temperature contour at year 30 of simulation. xz-plane cut.

The temperature contour in figure 4.3 displays a xz 2D plane cut at y = 200 m. Both boreholes ca be clearly shown by their relatively lower temperature compared to the surrounding bedrock. However, the influence of heat exchange quickly diminishes in the x-direction. Only a small difference in temperature of the bedrock around the boreholes can be seen. The figures are showing the state of the system after 30 years of continuous operation, which means the heat exchange has reached the semi-steady condition previously displayed.

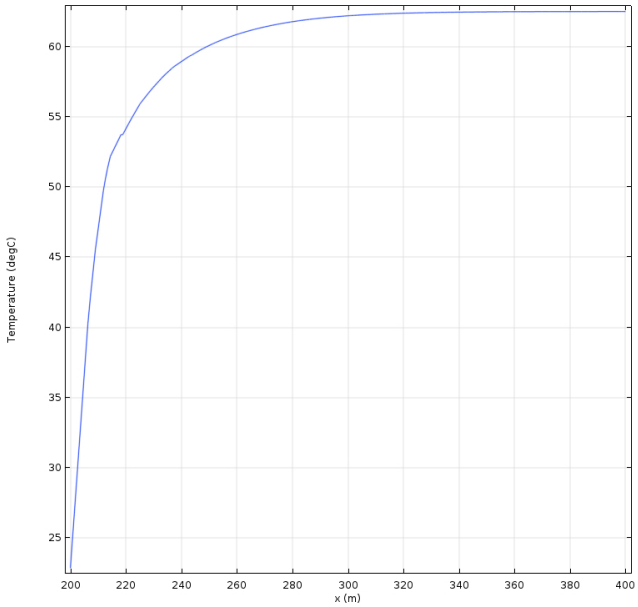

Figure 4.4: Temperature profile of bedrock in x-direction from borehole at depth 3500 m.

Figure 4.4 shows the temperature profile in positive x direction at 3500 m. At a distance of 100 m from the borehole, the bedrock is virtually undisturbed. Even 40 m from the borehole the temperature has almost reached the ambient condition. This signifies that the geometry in place is more than adequate to properly accommodate the simulations. It also shows that heat exchange from the surrounding bedrock is limited and that the bedrock is slow to compensate for the energy extraction of the boreholes.

4.3 Parametric sweep

For the parametric sweep, four characteristics parameters of the system is singled out and tested. These are fluid flow, incoming fluid temperature, pipe radius and thermal conductivity of the crystalline bedrock. These are all tested individually and the parameter value ranges are set to test the limits that the parameters have on the system.

4.3.1 Fluid mass flow

Fluid mass flows where run in the simulation from 1 kg/s to 35 kg/s.

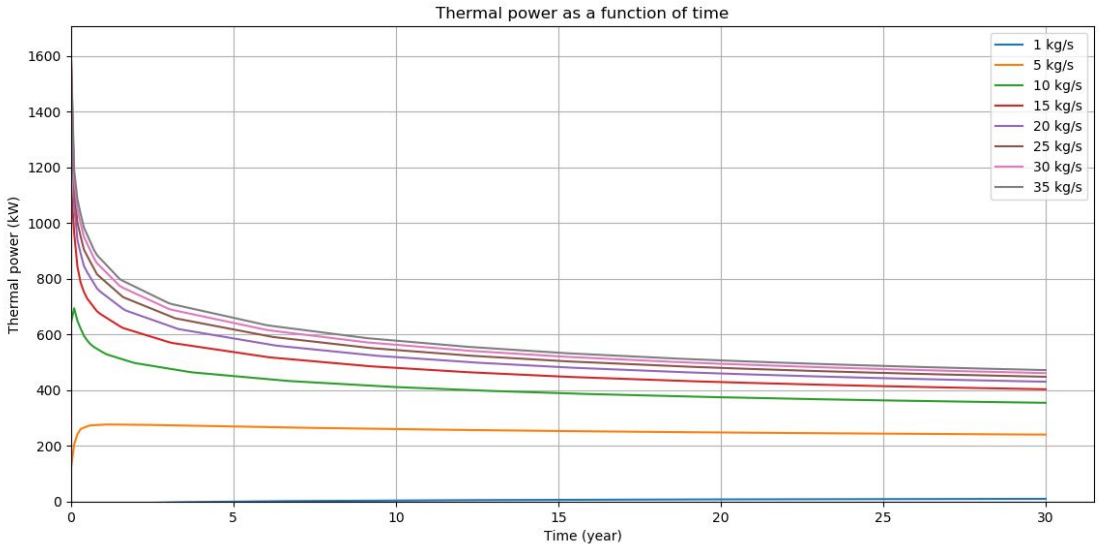

Figure 4.5: Thermal power (kW) as a function of time for varying fluid flow (kg/s).

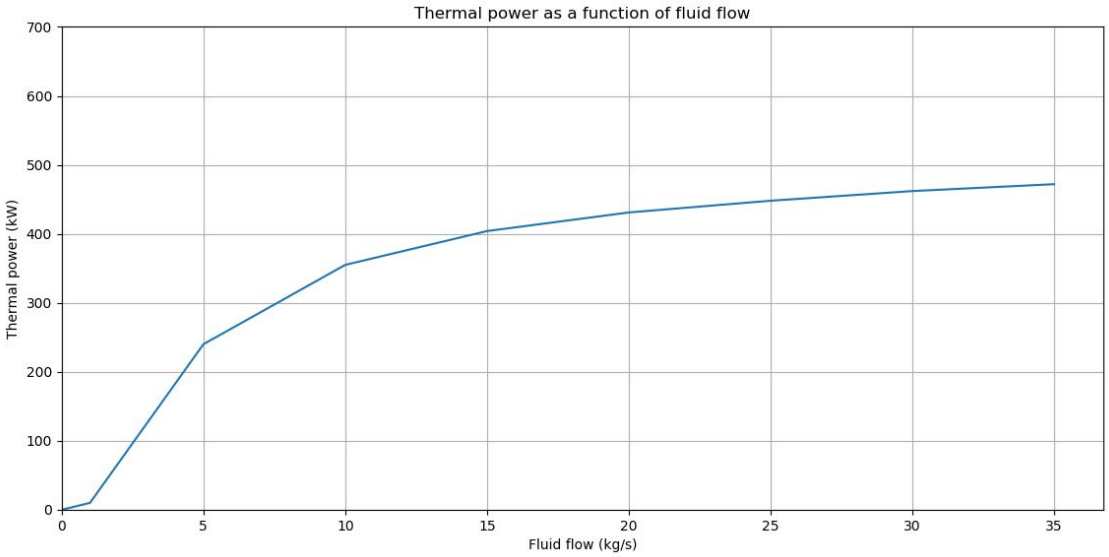

Figure 4.6: Thermal power (kW) as a function of fluid flow (kg/s) at year 30.

With increased fluid mass flow the system will experience a higher thermal power. As seen with 1 kg/s the thermal power remains steady and even increases slightly with time. However, close to 5 kg/s is a breaking point where the heat exchange is no longer sufficient to supply the fluid with energy at a constant flow. With higher fluid mass flows, the initial thermal power declines heavily for it to settle at a lower stable output. It is also clear that, the practice of increasing the fluid mass flow is a tactic with limited efficiency. As seen in figure 4.6, the thermal power converges towards 500 kW. In practical terms, increasing the fluid mass flow indefinitely is not an option. Pressure losses in the system will have to be taken into consideration from an operational standpoint. These losses contributes to the fluid temperature,

however since the heat comes from the electricity which drives the pump, it is not desirable.

Fluid flow (kg/s)\Year	0	1	5	10	20	30
1	-33	-10	0	4	8	10
5	117	276	270	261	248	241
10	640	542	452	412	375	355
15	1146	674	539	481	430	404
20	1477	754	588	520	460	431
25	1604	806	620	545	480	448
30	1623	845	644	564	495	462
35	1617	873	662	579	507	472

Table 4.1: Thermal power (kW) displayed for fluid flows (kg/s) over a few selected years.

A closer look at the thermal power of the different fluid mass flows shows that 1 kg/s has an increase thermal power from an initial negative output. The highest simulated flow sees a decline of 71 % from the initial value. For the higher fluid mass flows the change is, as previously stated, small. With an increase mass flow of 40 % from 25 kg/s to 35 kg/s, the thermal power only increases by 5.4 %.

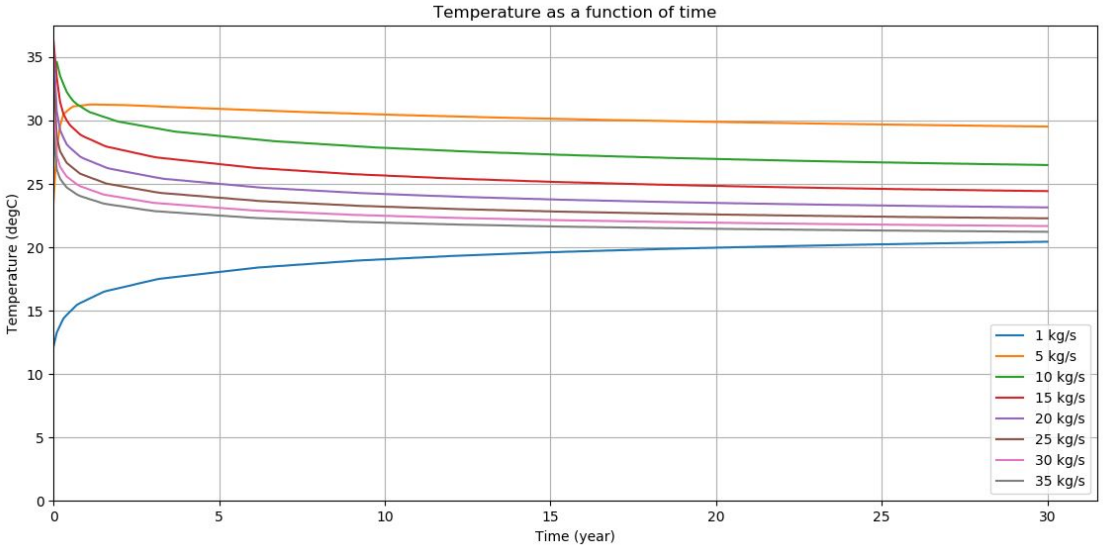

Figure 4.7: Outgoing fluid temperature ($°C$) as a function of time for varying fluid mass flow (kg/s).

Adding a graph displaying the temperature differences between the fluid mass flows, another picture emerges. Showing a similar pattern of figure 4.5, the graph displays mirrored results. A sufficiently low flow yields an outlier, as seen with fluid mass flow of 1 kg/s. Eliminating this value, the other flows show a pattern. The line representing 5 kg/s, with the weakest thermal power output, displays the highest exiting water flow temperature. Referring to the term representing the heat exchange

through the pipe wall, equation 2.10, the effect can be explained by temperature gradient. While the effective overall heat transfer coefficient regulates heat transfer, the dimensions of the system ensures an adequate area to negate this. The remaining part is the temperature difference between pipe fluid and the pipe surroundings. With an increased fluid mass flow, the influx of cool water lowers the borehole perimeter temperature at an increased rate, creating a higher temperature gradient along the length of the borehole. The fluid mass flow and the outflowing fluid temperature are working against each other. The thermal power is calculated by equation:

$$Q = \dot{m} C_p \nabla T \tag{4.1}$$

where Q (W) is thermal power, $\dot{m}$ (kg/s) is fluid mass flow, C_p $(J/(kg \cdot K))$ is specific heat capacity and ∇T (K) is temperature difference of inflowing and outflowing water. The temperature difference nullifies the fluid mass flow at higher flows.

4.3.2 Incoming fluid temperature

Incoming fluid temperatures are simulated from 0 $°C$ to 35 $°C$.

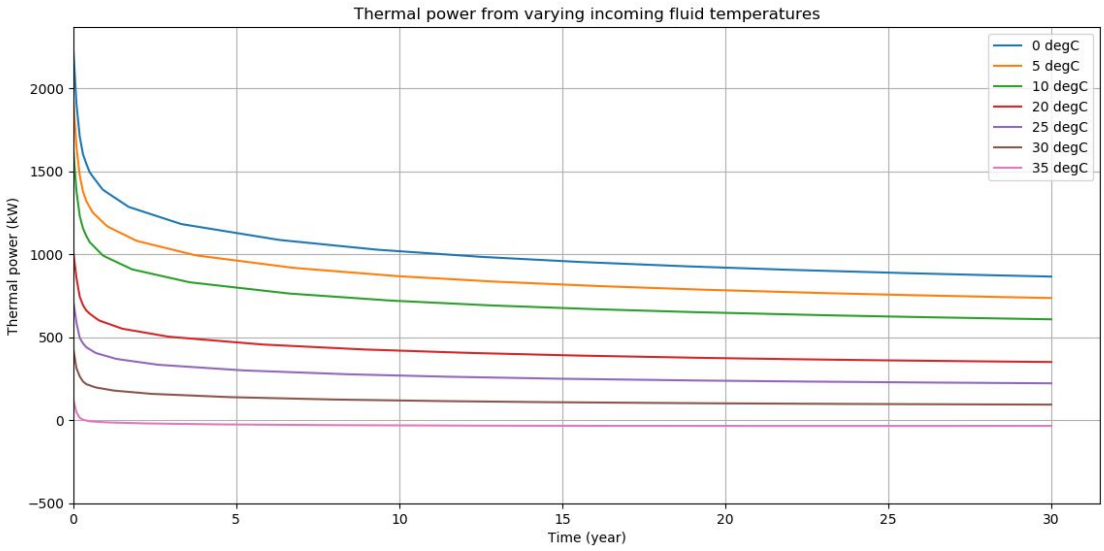

Figure 4.8: Thermal power (kW) as a function of time for varying incoming fluid temperature $(°C)$.

The thermal power shows an evenly spaced difference in output with temperature difference. The highest incoming fluid temperature ultimately deliver a negative energy balance, meaning the overall energy in the model increases. There is no indication for an upper limit to the possible thermal power output. However, in a real scenario, having a incoming fluid temperature below 0 $°C$ is problematic. As a standard practice, the fluid in geothermal applications are kept around 0 $°C$ as a minimum. This is to avoid erratic behavior due to phase change of the fluid and freezing of the ground around the borehole. For the purpose of a heat pump, a lower return temperature also negatively affects the coefficient of performance.

Incoming fluid temperature (degC)\Year	1	5	10	20	30
0	1392	1132	1021	921	867
5	1196	966	870	784	738
10	995	803	721	648	610
20	595	472	421	375	352
25	395	305	271	239	224
30	192	140	120	103	95
35	-10	-24	-30	-33	-33

Table 4.2: Thermal power (kW) displayed for incoming fluid temperatures ($°C$) over a few selected years.

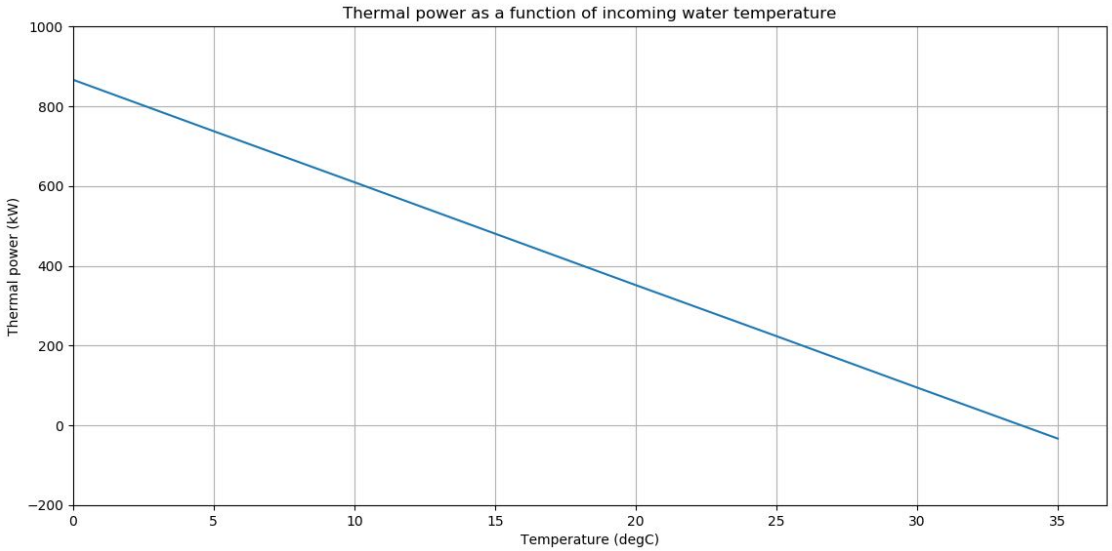

Figure 4.9: Thermal power (kW) as a function of incoming fluid temperature ($°C$) at year 30.

The thermal power extracted from the system has a linear relationship with incoming fluid temperature. At year 30 the difference is close to 130 kW for every 5 $°C$. The correlation is consistent, although the power difference narrows with time. In figure 4.9 the thermal power is displayed as a function of incoming fluid temperature. Around 34 $°C$ is the breaking point where the thermal power turn negative.

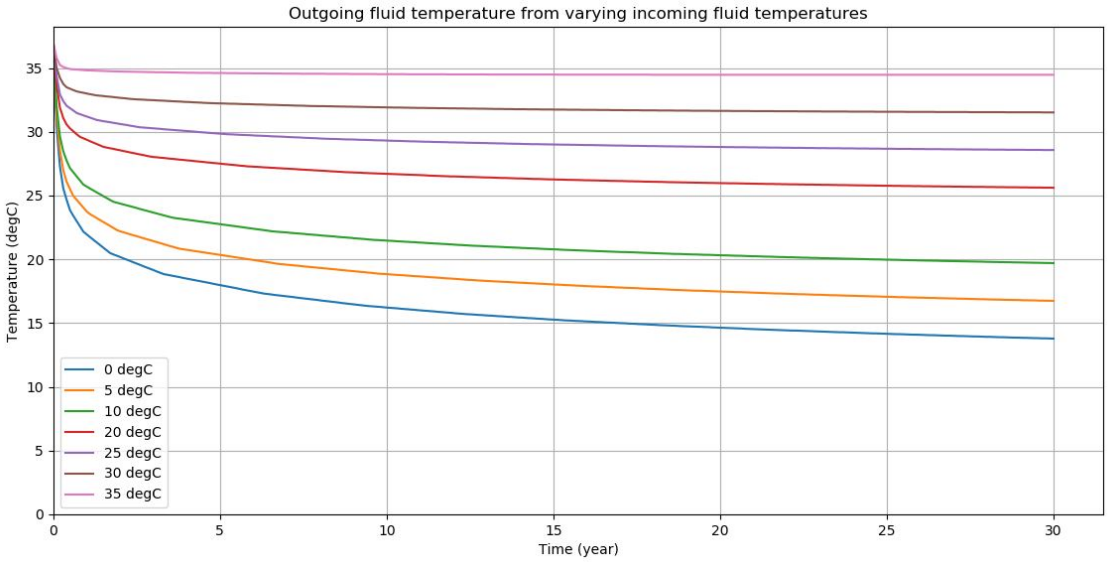

Figure 4.10: Outgoing fluid temperature ($°C$) as a function of time for varying incoming fluid temperatures ($°C$).

Temperature increase shows an evenly distributed pattern in figure 4.10. Lower temperature leads to higher thermal power as showed before, but at the same time the outgoing fluid temperature decreases.

Incoming temperature ($°C$)\Year	1	5	10	20	30
0	22.2	18	16.2	14.6	13.8
5	24.1	20.4	18.8	17.5	16.7
10	25.9	22.8	21.5	20.3	19.7
20	29.5	27.5	26.7	26	25.6
25	23.3	29.9	29.3	28.8	28.6
30	33	32.2	31.9	31.6	31.5
35	34.8	34.6	34.5	34.5	34.5

For every 5 $°C$ increase in incoming fluid temperature the outgoing temperature increase with 3 $°C$ at the 30 year mark. The energy equation of the borehole is equation 2.9. The source term for the heat exchange between the borehole and its surroundings is Q_{wall}. Besides the effective overall heat coefficient, it is the temperature gradient which dictates the heat exchange. Lowering the fluid temperature has a direct impact on this source term, explaining the higher thermal power output of the system. As shown in figure 4.2, the fluid experiences positive and negative heat exchange on its journey. Lower incoming temperature means that the positive exchange extends to a larger part of the borehole length.The surface temperature of the model is 10 $°C$, so incoming fluid temperatures below this value only experiences negative heat exchange on the way back to the surface.

4.3.3 Borehole radius

With an increased borehole radius, the heat exchanger area increases. Flow velocity is naturally affected by this, together with pressure loss due to friction. The radius is varied from 75 mm to 300 mm.

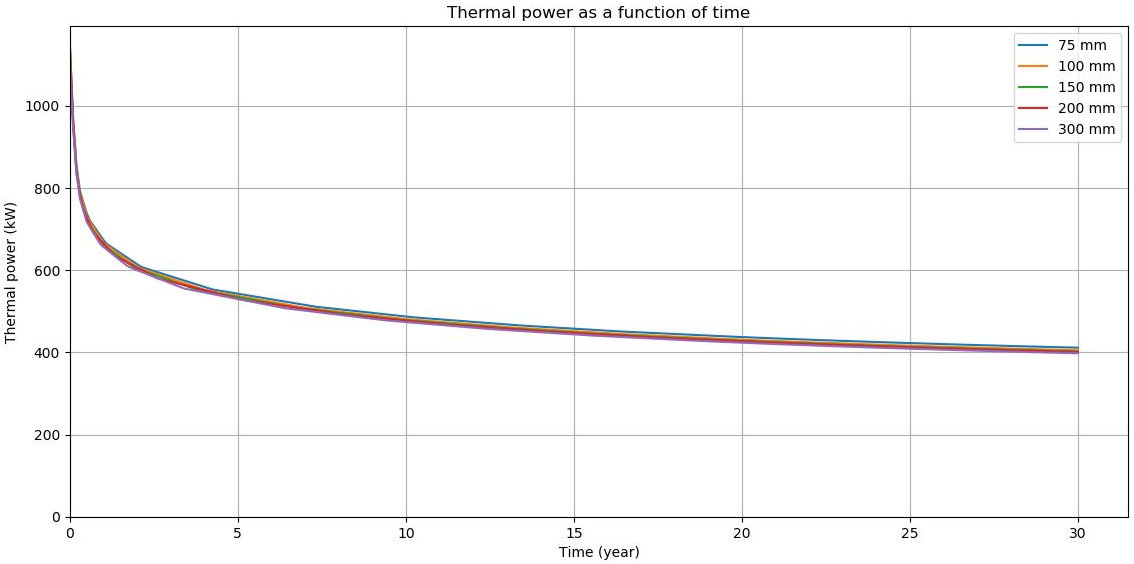

Figure 4.11: Thermal power (kW) as a function of time for varying pipe radius (mm).

Thermal power varies only slightly in preference of a smaller radius. With a radius of 300 mm the thermal power after 30 years is 398 kW and for 75 mm it is 412 kW. However, at the bottom turn the fluid temperature of the larger pipe radius is slightly higher at 23.4 $°C$ compared to the small pipe radius of 22.8 $°C$. The drop in thermal power can be connected to the higher flow velocity of the smaller pipe radius leaving less opportunity to lose heat on the return to the surface.

Heat exchanger area ranges from 3299 m^2 to 13 197 m^2 with little difference in result. What one can see from this parametric sweep of the pipe radius is that neither the pipe heat exchange area, nor the fluid velocity have a particularly important impact on the performance of the system.

4.3.4 Thermal conductivity

The thermal conductivity of the crystalline bedrock is examined for a range of values. Different from the other parameters this is a site specific condition. Thus in the design and construction of the geothermal system this value is set and unable to change, except from choosing a location with preferable bedrock properties. The thermal conductivity range goes from 1 $W/(m \cdot K)$ to 8 $W/(m \cdot K)$.

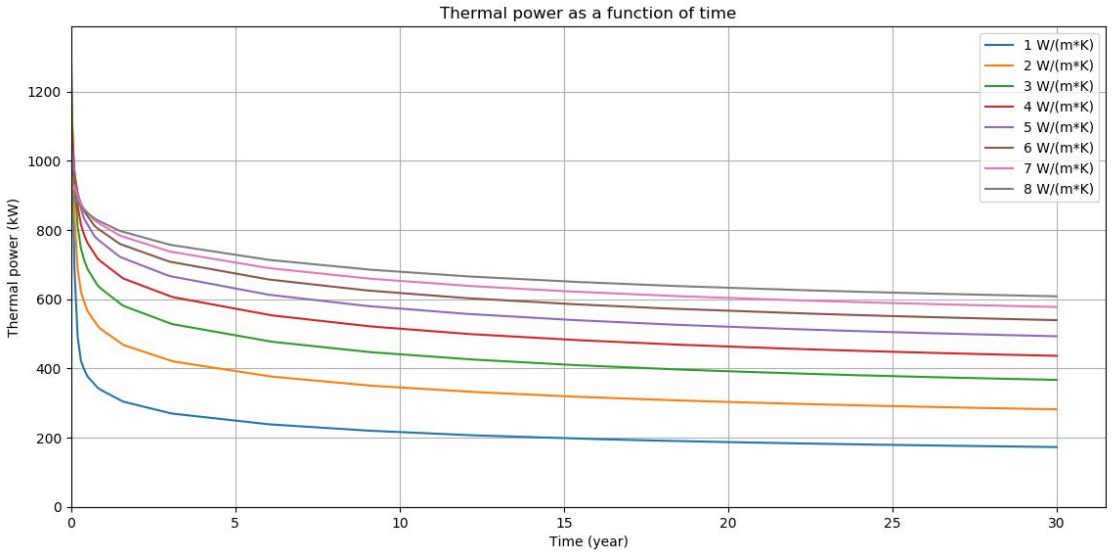

Figure 4.12: Thermal power (kW) as a function of time for varying thermal conductivity ($W/(m \cdot K)$) for crystalline bedrock.

Increased thermal conductivity shows a positive impact on thermal power output. This is the only change which has shown a consistent positive outcome over both temperature and thermal power. For 1 $W/(m \cdot K)$ the thermal power is 173 kW and 20.8 $°C$, to the highest of 8 $W/(m \cdot K)$ with 609 kW and 27.7 $°C$. With an increase in thermal conductivity it is clear that the surrounding bedrock is capable of providing a higher rate of heat flux. Looking back at eq 2.20 the thermal conductivity k is the driving force to heat exchange together with temperature gradient.

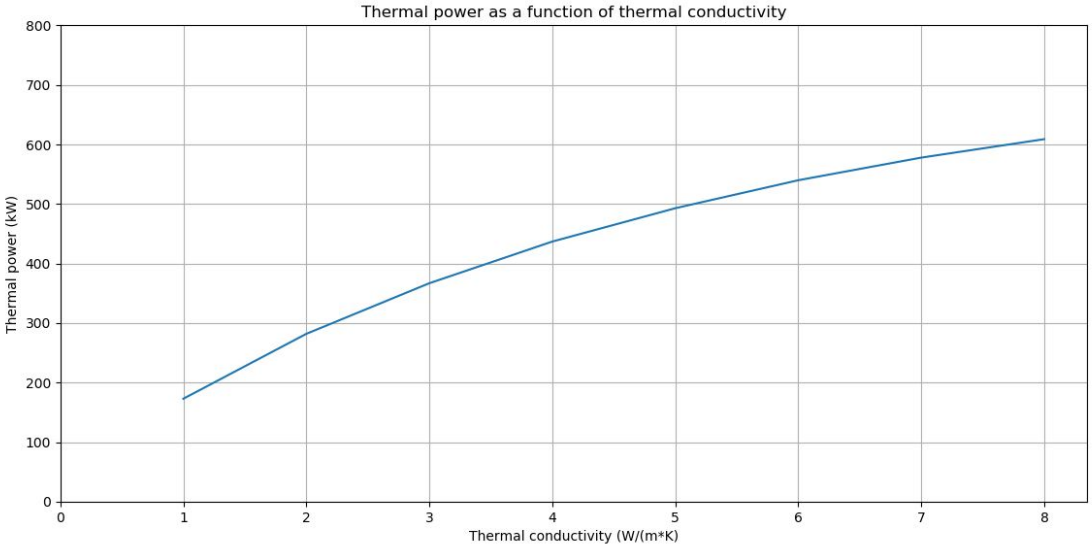

Figure 4.13: Thermal power (kW) as a function of thermal conductivity ($W/(m \cdot K)$) of crystalline bedrock at year 30.

Thermal conductivity increases thermal power significantly. However, the efficiency of the increase is not linear, but shows a small decline in efficiency.

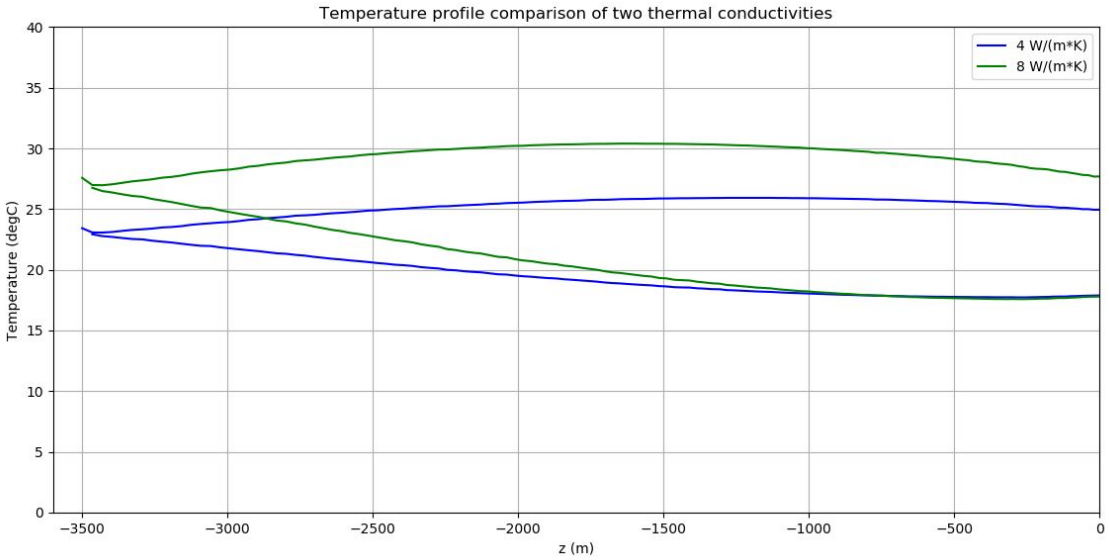

Figure 4.14: Temperature profile comparison between thermal conductivity of 4 and 8 $(W/(m \cdot K))$.

A closer look at two temperature profiles with thermal conductivity of 8 respectively 4 $(W/(m \cdot K))$ shows that maximum temperature for the green curve is 30.4 $°C$ at -1596 m and for the blue curve it is 25.9 $°C$ at -1231 m. This means the fluid starts to lose heat above those levels. The lower value of thermal conductivity gives a longer distance where positive heat exchange occurs. This explains the slowly declining efficiency of higher thermal conductivity. With high heat exchange to the borehole, the fluid reaches a higher temperature but it is also limited in the return to the surface. For an effective system, the return borehole would need to be isolated to a certain depth depending on rock properties.

5
Conclusion

In this study two categories were in focus, design/operating parameters and thermal properties of the bedrock. The design parameters included fluid mass flow, incoming water temperature and borehole radius. The thermal properties of bedrock consisted of thermal conductivity.

Useful energy drops significantly in the first few simulated years, before it reaches a semi-stable level after the first decade. After this point, output change has a weak correlation with time, although the decline does not cease completely. It is shown in the results, that extracted thermal power is all but constant over time, even after 50 years, as displayed in figure 4.1. Over the different simulations this pattern is constant, meaning you can not count on a steady flow of power and it especially fluctuates in the first ten years. This raises an issue in calculating the possible profits one might yield from a geothermal system of this kind.

The sensitivity analysis of the design and operational parameters showed a restraint in the system. From the energy equation 2.9 used in COMSOL Multiphysics, the term of importance is the heat source term, defining the heat exchange between the borehole and its surroundings:

$$Q_{wall} = (hZ)_{eff}(T_{ext} - T) \tag{5.1}$$

The state of the system can in part be explained by this. The driving force of the heat exchange is the temperature difference between the pipe fluid and the surrounding environment. Given the length of the boreholes, an adequate heat transfer area is provided. That is clearly shown in the parametric sweep of the borehole radius, where the smallest radius gave 3299 m^2 of surface area while the largest provided 13 197 m^2. The case was further established by the slightly favourable thermal power of the smaller radius. Left is the temperature gradient. Parametric sweeps of the parameters fluid mass flow and incoming fluid temperature, showed that both were limited by the temperature gradient.

Both cases showed an initial rapid decline in thermal power output and temperature in the borehole, which eventually lead to a semi-stable result. Fluid mass flow had moderate impact on the results, showing that a correlation of thermal power to Reynolds number was negligible. The slightly higher thermal power of increased

fluid flow, can be connected to the cooling of the borehole, leading to a higher temperature gradient.

Incoming fluid temperature therefore has a direct impact on the heat exchange between the borehole and its surroundings. A higher temperature gradient leads to a higher thermal power. However, there are limitations to the temperature range. In shallow geothermal heat pumps it is standard practice to keep the lower limit of the return temperature to 0 $°C$. This is to prevent erratic behaviour of the soil and water around the freezing point at atmospheric pressure. However, the reason for drilling deeper into the crust is to reach bedrock with higher temperature, and thus be able to extract water with higher temperature. The COP for a heat pump decreases with lower water return temperature. To return water from the heat pump to the borehole at 0 $°C$ would mean that the heat pump would not operate any more efficiently than a shallow geothermal heat pump. This would remove the need for deep drilling and ultimately an array of shallow boreholes could replace the former solution. For the current system with a depth of 3500 m and the temperature gradient of 0.015 K/m, this turns into an optimization problem. The return water temperature should be kept at a level where the COP of the heat pump is balanced against the thermal power output of the system. Electricity cost for driving the heat pump is a determining factor in this comparison. There is also an upper limit to take into consideration with return water temperature from the heat pump to the borehole. With a higher fluid temperature, the temperature gradient to the bedrock decreases until it is unable to maintain an overall positive heat exchange. This is especially true with a deep geothermal system where the depth of the system ensures a high difference in temperature along the boreholes. The fluid experiences a negative heat exchange in the upper part of the bedrock as seen in figure 4.2. Higher incoming temperature increased heat loss for both down- and upflowing fluid. As stated, the higher return water temperature ensures a preferable COP but lowers the thermal power extracted from the bedrock.

As stated the temperature gradient between borehole and bedrock dictates the heat exchange between the two. It is explained that the convective heat exchange in the borehole is more than adequate to saturate the system. Left is the conductive heat exchange in the bedrock. The physics regulating energy balance in the bedrock is shown by Eq 2.20.

$$\rho C_p \frac{\partial T}{\partial t} - \nabla \cdot (k \nabla T) = 0 \tag{5.2}$$

Rearranging it and neglecting the heat source term:

$$\frac{\partial T}{\partial t} = \frac{\nabla \cdot (k \nabla T)}{\rho C_p} \tag{5.3}$$

The temperature change with the respect to time is dependent on the dissipation of heat in the bedrock. This is measured by thermal diffusivity m^2/s:

$$a = \frac{k}{\rho C_p} \tag{5.4}$$

Where k ($W/(m \cdot K)$) is thermal conductivity, ρ (kg/m^3) is density and C_p ($J/(kg \cdot K)$) is specific heat capacity. The product of density and specific heat capacity is often referred to volumetric heat capacity $J/(m^3 \cdot K)$. It describes the ability of a defined volume of a material to store internal energy with temperature change. The crystalline bedrock used in the model is granite with a density of 2600 kg/m^3, specific heat capacity of 850 $J/(kg \cdot K)$ and thermal conductivity of 3.5 $W/(m \cdot K)$. The thermal diffusivity is then 1.6 mm^2/s. To put that into perspective the thermal diffusivity of iron is 23 mm^2/s. The thermal diffusivity is also a measure of thermal inertia ($J/(m^2 \cdot K^1 \cdot s^{1/2})$) which consists of the same properties:

$$I \equiv (k\rho C_p)^{1/2} \tag{5.5}$$

Thermal inertia describes how slowly the temperature of an object reaches that of its surroundings. It therefore measures the responsiveness a material has to change in temperature. Generally, crystalline rock is dense and has a relatively high thermal inertia, which is true for the granite rock used in the model. The thermal inertia is 2781 ($J/(m^2 \cdot K^1 \cdot s^{1/2})$). The combination of a high thermal inertia and low thermal diffusivity creates a situation where heat is conducted poorly. The volumetric heat capacity dominates the thermal diffusivity equation. All of this creates a system which responds slowly. The heat penetration is low as displayed in figure 4.4.

There are three important points to take out from this analysis. First is that the convection in the boreholes will be sufficient to satisfy the necessary heat exchange with the borehole perimeter. The second point is the temperature gradient between the fluid and the surrounding bedrock. This dictates the heat exchange for the boreholes. This parameter has some flexibility and with a lower incoming fluid temperature you will have a higher thermal power. However, there is a trade of with lower temperature of the outgoing water, making this less appealing in a heat pump. The third point and the most important factor to take into consideration, is the conduction in the bedrock. It is clear that the limitation of thermal power is highly connected to this property. The high thermal inertia with a low thermal conductivity leads to a slow response from the rock. Unfortunately, this situation is unchangeable and primary effort should be given to find a way of expanding the surface area with the rock.

The potential of HDR makes it an important step in gaining an abundant energy source with minimal environmental impact. Unfortunately, too little research has been done to shed light on this matter, and make HDR a reliable alternative to conventional technology. As mentioned in Section 1.1, the focus of investigation thus far has been in "engineered" geothermal HDR systems. This means the method of using hydraulic fracturing or chemical enhancement of fractures in the bedrock to allow for water to flow between two wells. With all the uncertainty that comes with this technique[20], the need for investigating alternatives is clear. For that purpose a closed loop geothermal system was evaluated in this Master's Thesis. Modelled with the same conditions as one would expect for conventional HDR, with the aim

of exploiting the higher temperature hidden in deep crystalline bedrock.

With the general conditions that is typical for Sweden, a closed loop deep geothermal system has been modelled and evaluated. However, the scope of the results is not necessarily confined to Sweden alone. The technique for drilling and constructing geothermal systems must be considered universal. The design of the system can easily be implemented under other circumstances. The differences encountered, is limited to the properties of the bedrock such as thermal conductivity and local temperature gradient with depth.

Bibliography

[1] Dumas P. Perspectives for Geothermal Energy in Europe. Chapter 1, 2017.

[2] Batchelor A.S. Progress in Hot Dry Rock Exploitation. U.K, Cornwall TRlO SOU, Rosemanowes Quarry Herniss, Penryn. Camborne School of Mines Geothermal Energy Project, 1985.

[3] Barbier E. Geothermal energy technology and current status: an overview. Pisa: Institute of Geosciences and Earth Resources, Area della Ricerca del CNR, Via Moruzzi 1, 56124, 2002.

[4] National Research Council. Drilling and Excavation Technologies for the Future. Chapter 7, 1994.

[5] Ghassemi A. A Review of Some Rock Mechanics Issues in Geothermal Reservoir Development. 2012.

[6] Brown D.W. Mining the Earth's Heat: Hot Dry Rock Geothermal Energy. 2012.

[7] Watson, A. Geothermal Engineering: Fundamentals and Applications. 2013. pp 25-66.

[8] Barnard, C.L. et al. A Theory of Fluid Flow in Compliant Tubes. vol 6, 1966. pp 717–724.

[9] Lurie M.V. Modeling of Oil Product and Gas Pipeline Transportation. 2008.

[10] White, F.M. Fluid Mechanics. New York: McGraw-Hill, 7th edition, 2011.

[11] Incropera, Frank P. Principles of heat and mass transfer. 7th edition, 2013. pp 518-567.

[12] Tullborg E., Larson S. Porosity in crystalline rocks – A matter of scale. 2005.

[13] Sundberg, J. Termiska egenskaper i jord och berg. 1991.

[14] Cho W.J., Choi J.W., Kwon S. The thermal conductivity for granite with various water contents, Engineering Geology. ENG GEOL, 2009. pp 107, 167-171. 10.1016/j.enggeo.2009.05.012.

[15] Eppelbaum L., Kutasov I., Pilchin A. Applied Geothermics. Chapter 2, 2014.

[16] COMSOL. Pipe Flow Module User's Guide. 2012.

[17] Dijkshorn L., Speer S., Pechnig R. Measurements and Design Calculations for a Deep Coaxial Borehole Heat Exchanger in Aachen, Germany. 2013.

[18] Kohl, T., Brenni, R., Eugster, W. System performance of a deep borehole heat exchanger. vol 31, no 6, 2002. pp 687–708.

[19] Tuomas G. Water Powered Percussive Rock Drilling.

[20] Haraden J. The Status of Hot Dry Rock as an Energy Source. Energy Vol 17, No 8, 1992. pp 777-786.